Supplementary materials

Nanoflower-like Co_3S_4/FeOOH/NF Heterostructure for Enhanced Peroxymonosulfate Activation: Synergistic Radical and Non-Radical Pathways toward Efficient Norfloxacin Degradation

Yuerong Zhou, Ming Yi, Yu Zhao, Rui Yang, He Yan, Xiuwen Cheng*

Key Laboratory for Environmental Pollution Prediction and Control, Gansu Province, College of Earth and Environmental Sciences, Lanzhou University, Lanzhou, 730000, P.R. China

***Corresponding author address:**

Prof. & Dr. Xiuwen Cheng

College of Earth and Environmental Sciences, Lanzhou University, Lanzhou 730000, China

E-mail: chengxw@lzu.edu.cn (X. Cheng)

Revision resubmitted to

Frontiers of Environmental Science & Engineering

Nov., 2025

Supplementary Information

Text S1. Chemicals and reagents

The chemicals and reagents used in this study were analytical grade, including: ferric chloride hexahydrate ($FeCl_3 \cdot 6H_2O$) was purchased from XiLong Scientific Co., Ltd. (Guangdong, China). Sodium hydroxide (NaOH), sodium thiosulfate pentahydrate ($Na_2S_2O_3 \cdot 5H_2O$), potassium nitrate (KNO_3), methanol (MeOH), tert-butanol (TBA) and hydrochloric acid (HCl) were purchased from Damao Chemical Reagent Co. Ltd (Tianjin, China). Sodium dihydrogen phosphate (NaH_2PO_4), potassium chloride (KCl) , sodium azide (NaN_3) and ascorbic acid (AA) were supplied by Sinopharm Chemical Reagent Co. Ltd (Shanghai, China). Potassium bicarbonate ($KHCO_3$) was purchased from Kermel Chemical Reagent Co. Ltd (Tianjin, China). cobalt chloride hexahydrate ($CoCl_2 \cdot 6H_2O$), 5,5-Dimethyl-1-pyrroline- N-oxide (DMPO) and 2,2,6,6-tetramethyl-4-piperidone (TEMP), p-benzoquinone (p-BQ), peroxymonosulfate (PMS, $KHSO_5 \cdot 0.5KHSO_4 \cdot 0.5K_2SO_4$), were purchased from Aladdin Chemistry Co., Ltd (Shanghai, China). Wahaha (Hangzhou, China) deionized water was applied throughout the experiments.

Text S2. Characterization

X-ray diffraction (XRD) analysis was conducted on a Rigaku Ultima IV diffractometer using Cu Kα radiation (λ = 0.1541871 nm) with a scanning range of 10°–80° (2θ) at a step size of 0.02° and a scan rate of 10° min^{-1}. Electrochemical tests were carried out on a CHI 660e workstation (Shanghai Chenhua Instruments, China) using a standard three-electrode setup. In-situ grown NF-supported catalyst served directly as the working electrode, while a Pt plate and Ag/AgCl electrode served as the counter and reference electrodes, respectively, with 0.3 g/L PMS as the electrolyte. The morphology, crystal structure and elemental composition of the samples were analyzed using scanning electron microscopy (SEM, Apero S, USA) and transmission electron microscopy (TEM, Talos F200C, USA), both equipped with Energy Dispersive X-Ray spectroscopy (EDS). Reactive oxygen species in the reaction were detected by electron paramagnetic resonance spectroscopy (EPR, Bruker ER200DSRC10/20, Germany). X-ray photoelectron spectroscopy (XPS) measurements were conducted using a Kratos AXIS Ultra DLD (Britain) instrument, with all data referenced to the C1s peak=284.8 eV for calibration. The point of zero charge (pH_{pzc}) was determined by the pH drift method. Briefly, a piece of Co_3S_4/FeOOH/NF was added to 50 mL of a 0.01 M NaCl solution. The initial pH was adjusted between 3.0 and 12.0 using 1 M NaOH or HCl. The suspensions were purged with N_2 for 5 min to eliminate carbonate interference, sealed, and then equilibrated at 25 °C for 48 h with shaking. The final pH was recorded, and the pH_{pzc} was identified as the point where the curve of ΔpH versus the initial pH crossed zero.

The liquid chromatography tandem mass spectrometry (LC-MS) was employed for the identification of intermediate products during NOR degradation. The C18 column (2.1*100 mm, 3 um) was adopted for chromatographic separation. The mobile phase

was a mixture of ultrapure water and acetonitrile in varying ratios at a flow rate of 0.3 mL/min, and the elution program is shown in Table S1 below.

Table S1. Mobile Phase Ratio (Ultrapure Water: Acetonitrile) (%) for determining NOR degradation intermediate using LC-MS.

Ratio (H_2O:ACN)	**Time (min)**
90:10	0 – 5
90:10 → 10:90	5 – 15
10:90	15 – 20
10:90 → 90:10	20 – 20.1
90:10	20.1 – 25

Methanol (MeOH), *tert*-butyl alcohol (TBA), p-benzoquinone (p-BQ), sodium azide (NaN_3), furfuryl alcohol (FFA), ascorbic acid (AA) were selected as scavengers for $SO_4^{\bullet-}$ and $^{\bullet}OH$, $^{\bullet}OH$, $O_2^{\bullet-}$,$^1O_2$, $^1O_2$ and all ROSs, respectively.

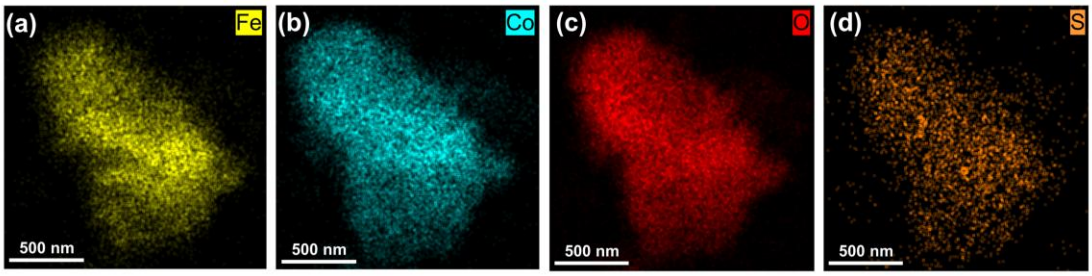

Fig.S1. TEM-EDS elemental mapping of Co_3S_4/FeOOH/NF.

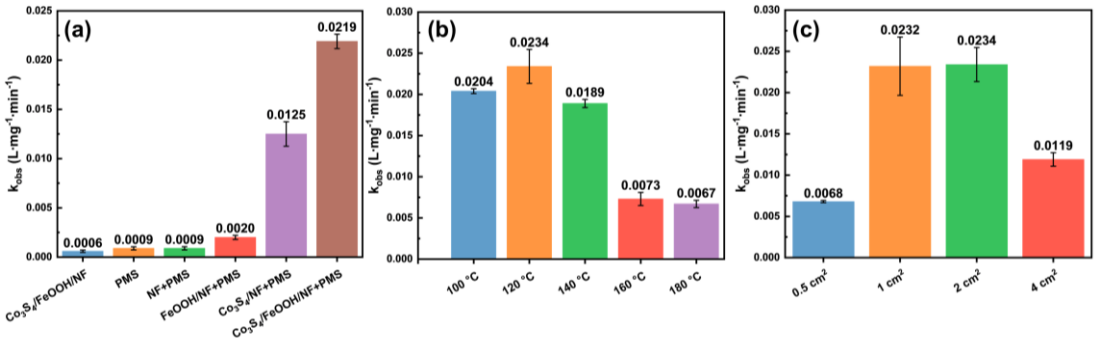

Fig.S2. Comparison of the pseudo-second-order rate constants (k_{obs}) for NOR degradation under different conditions: (a) catalytic systems, (b) hydrothermal temperature and (c) catalyst dosage.

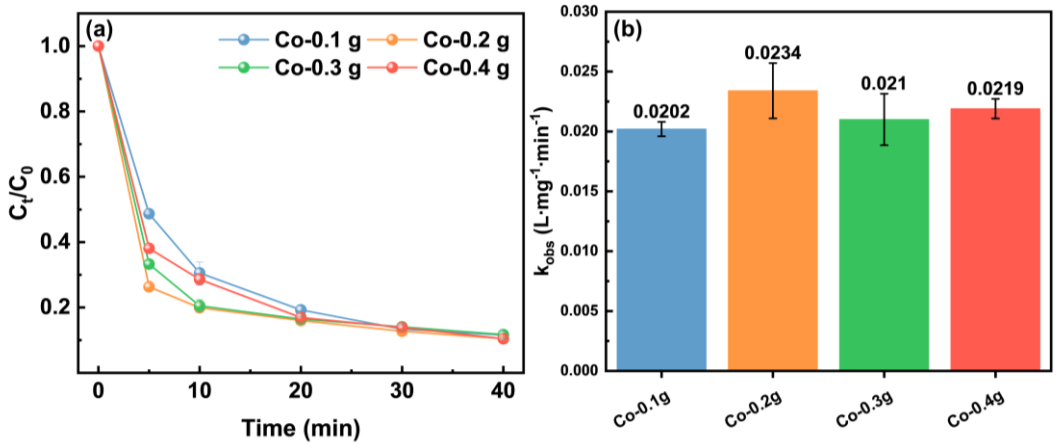

Fig.S3. The effect of Co addition in hydrothermal synthesis on NOR (a) degradation and (b) rate constant.

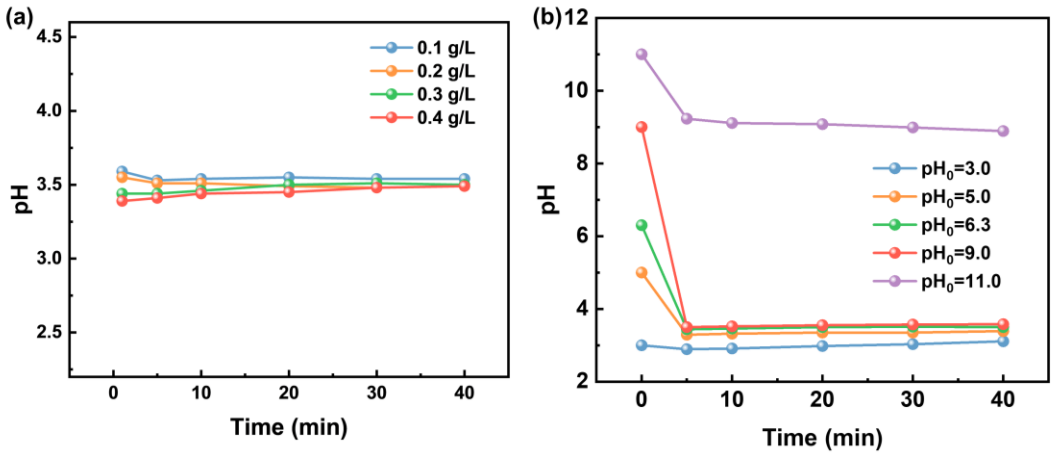

Fig.S4. (a) pH trends initiated from different initial values and (b) pH trends under different PMS concentrations during NOR degradation.

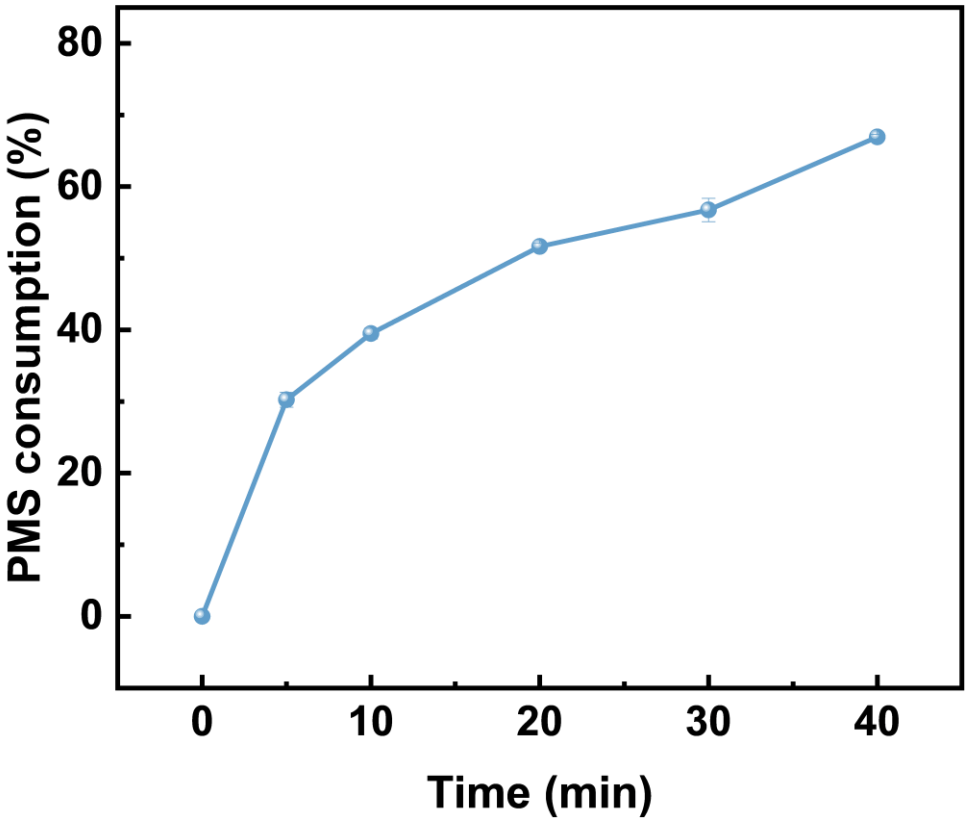

Fig.S5. Evolution of PMS consumption percentage during the catalytic reaction.

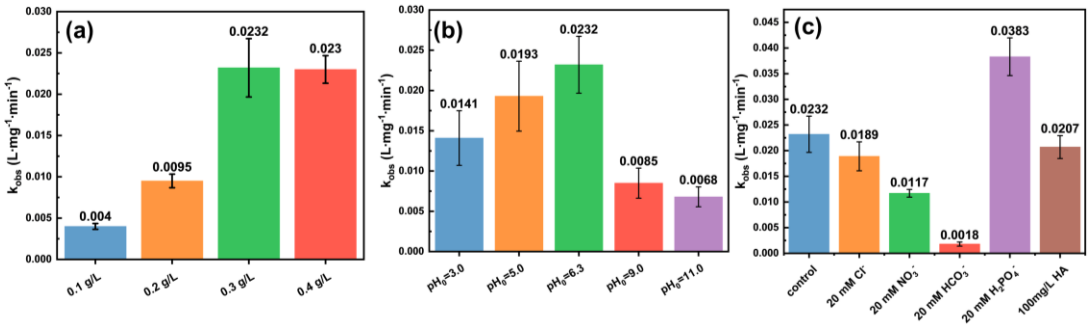

Fig.S6. Comparison of the pseudo-second-order rate constants (k_{obs}) for NOR degradation under different operational parameters: (a) PMS concentration, (b) initial pH value and (c) different co-existing substance .

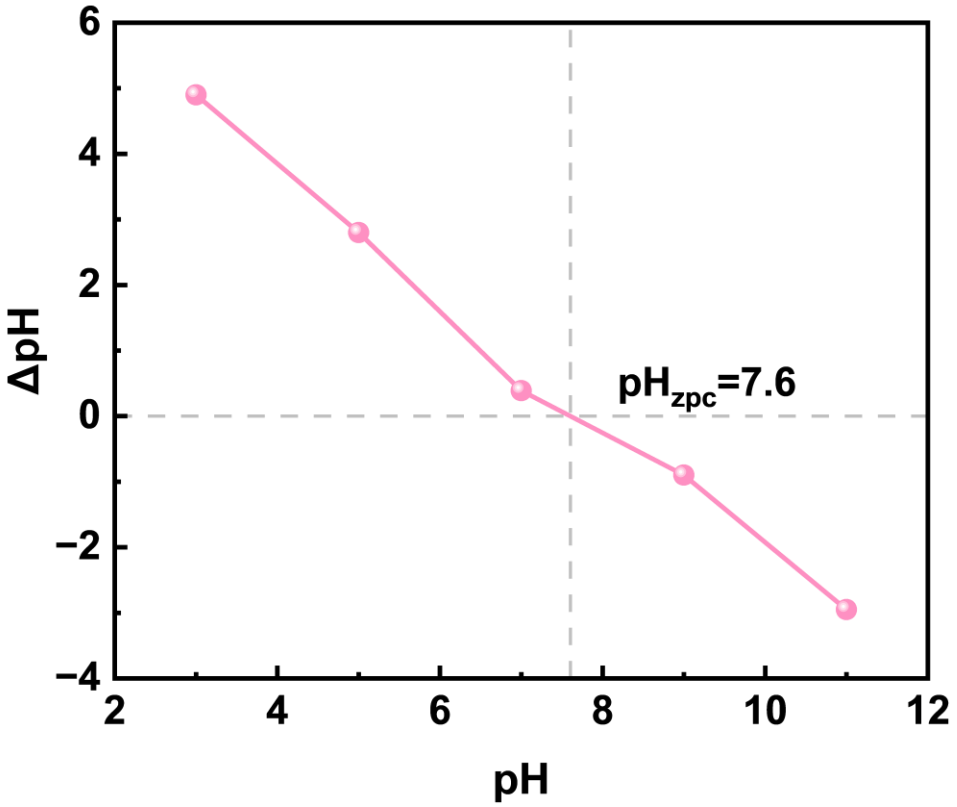

Fig.S7. pH_{pzc} plots for Co_3S_4/FeOOH/NF.

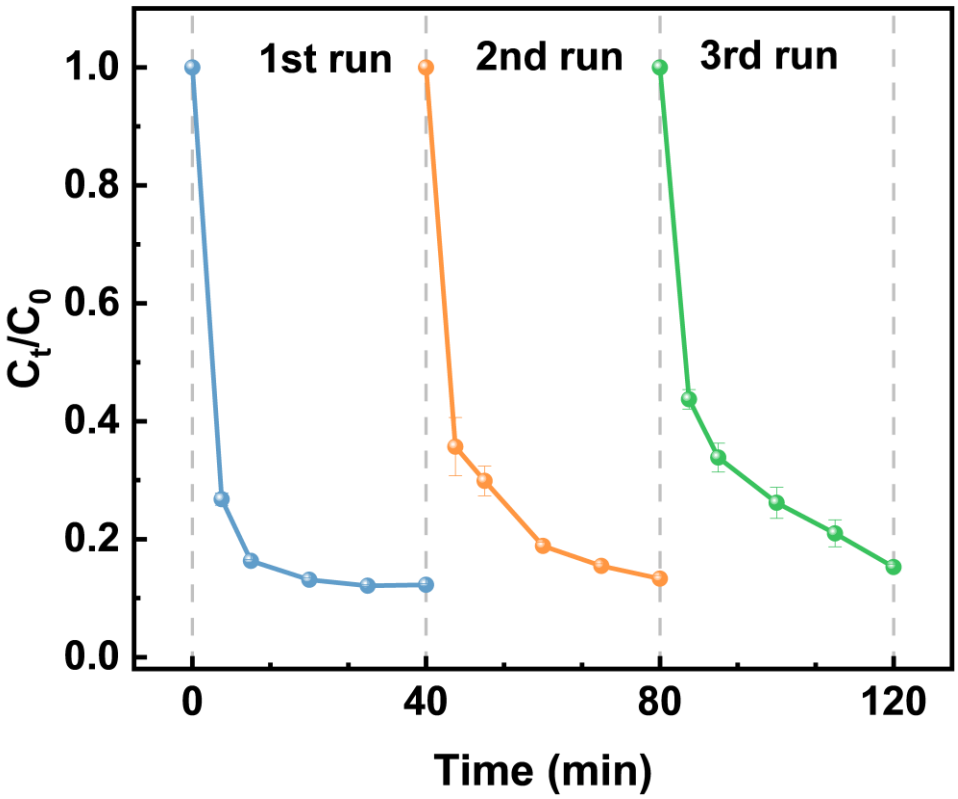

Fig.S8. Reusability of Co_3S_4/FeOOH/NF in activating PMS for NOR degradation.

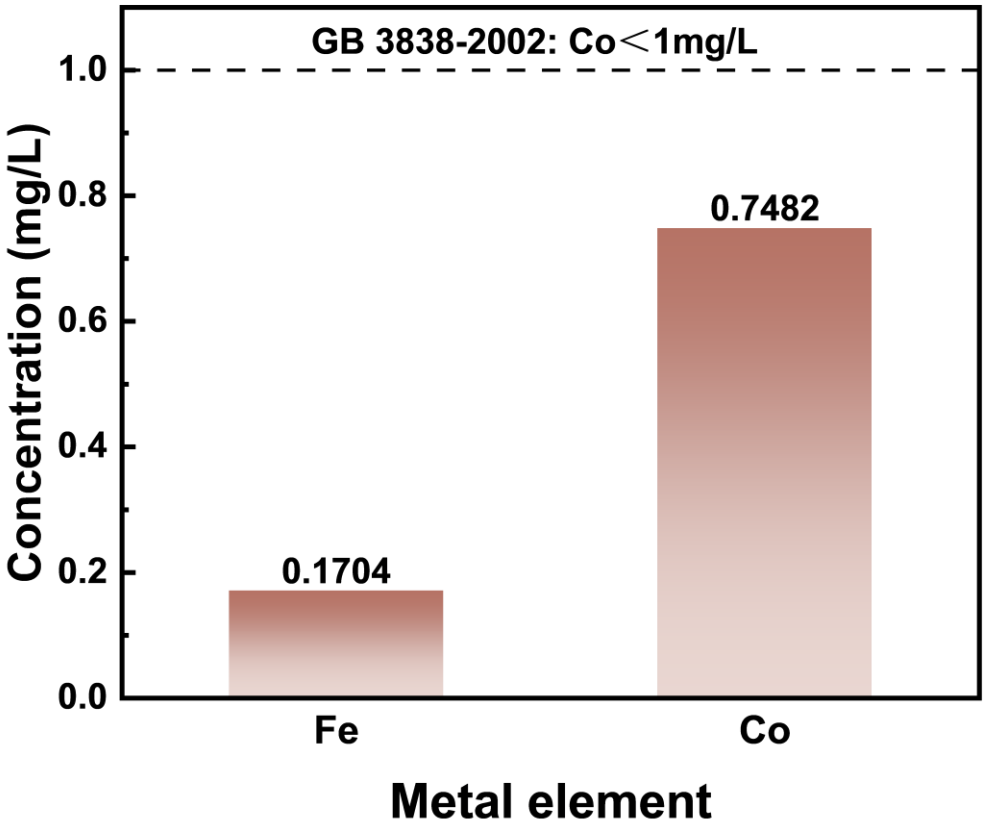

Fig.S9. Metal leaching of Fe, Co after the catalytic reaction for Co_3S_4/FeOOH/NF&PMS system.

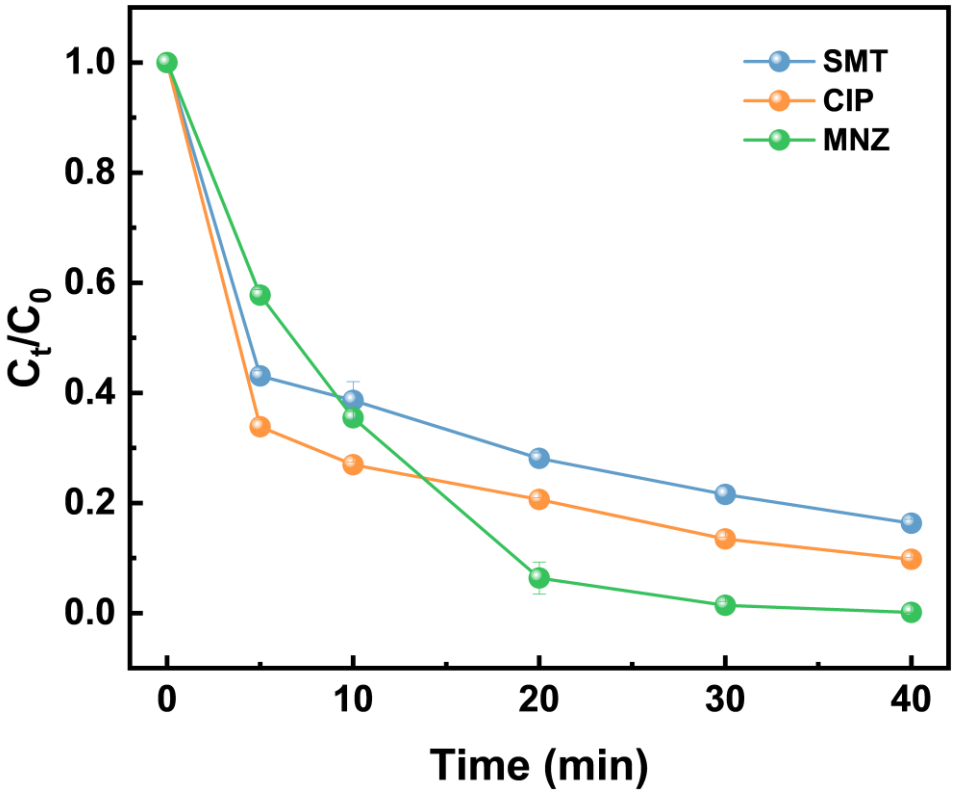

Fig.S10. Degradation of various antibiotics by the Co_3S_4/FeOOH/NF&PMS system.

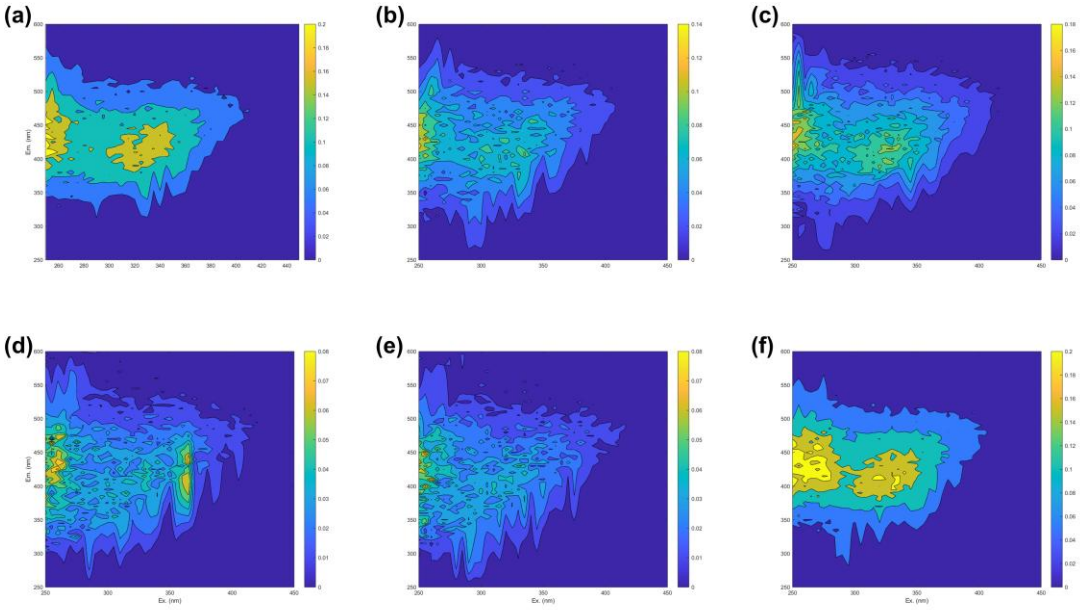

Fig.S11. 3D EEM spectra of real secondary sedimentation tank effluent in a wastewater treatment plant treated by Co_3S_4/FeOOH/NF&PMS system at (a) 0 min, (b) 5min, (c) 10 min, (d) 30 min, (e) 40 min, and (f) PMS system at 40 min.